THE USE OF A REAL-GAS POTENTIAL APPROACH IN A SIMULATOR FOR HIGHLY FRACTURED RESERVOIRS

W. Neal Sams[1], Duane H. Smith[2]

[1]EG&G, [2]DOE, National Energy Technology Laboratory (NETL), Morgantown, WV 26507-0880 U.S.A.

ABSTRACT

Dual-porosity simulators are ubiquitously used for fractured reservoirs. However, explicit-fracture simulators may be able to increase the accuracy and reliability of simulations for highly fractured reservoirs, because they can directly use descriptions (i.e., lengths, orientations, and apertures) of fractures as obtained from well logs (especially, fmi), outcrop analyses, and other geological data. Al-Hussainy, et al. (1966a, b) developed the real gas potential primarily for use in gas-well testing analyses and in single-phase simulators for a single, dry gas. The real gas potential is used in the current work to develop an explicit fracture reservoir simulator for fluids. This simulator considers flow through explicitly defined fractures as well as storage/recharge in/from the surrounding rock matrix. It considers the thickness, permeability, and porosity of the rock matrix. Each of the fractures contained in the reservoir has independently defined physical properties such as length, orientation, and aperture. As a result of the explicit handling of fractures as well as the use of the potential formulation, simulation of reservoirs containing tens of thousands of fractures can be performed in shorter times than those required by finite element codes.

1. INTRODUCTION

One approach to modeling flow in a naturally fractured reservoir has been to use an anisotropic permeability tensor along with finite elements (e.g. Park et al., 2002). An alternative approach is to explicitly incorporate fractures into the reservoir model. Beginning in the late 1970s, investigators of fractured aquifers began to statistically describe fracture networks for purposes of flow simulation. Initial attempts were simple. Networks were generated in a Boolean process in which fractures were randomly located and fracture length, aperture, and orientation were assigned as either fixed variables or as members of simple statistical distributions (i.e., uniform distributions, Gaussian distributions, or lognormal distributions) (see, e.g., Baecher et al., 1977). Flow simulation of these discrete irregular networks began during the early 1980s and was limited to small numbers of fractures that carried flow under steady-state conditions without matrix participation (e.g., Long et al., 1982).

Throughout the 1980s, development of irregular fracture network generators and flow simulators accelerated. This decade saw the advent of three-dimensional modeling, spatial correlation, flow simulation via several techniques, and contaminant transport modeling. Most of the computer programs, however, implemented aquifer models designed for investigation of either proposed radioactive waste repository sites or geothermal hard-rock reservoirs. More useful programs for modeling petroleum reservoirs appeared during the 1990s (e.g., new versions of FRACMAN by Golder Associates; hierarchical modeling of fracture networks in stratified

rock by Gervais et al. (1992); application of the pseudopotential for compressible flow, McKoy and Sams (1997)).

Networks and fractures themselves usually present large permeability anisotropies and heterogeneities across a range of scales. Thus, the scale of observation and spatial variability become critical issues in every investigation, and simple averaging, as required by conventional models, tends to loose utility.

NFFLOW a simulator that treats flow from a fracture network and its recharge from the surrounding rock has been developed for reservoirs of either gas or liquid. It computes transient flow rates or bottom hole pressures according to user specified pressure or rate schedules. It assumes that the reservoir is isothermal, that the reservoir is one layer, and that no flow across the upper and lower boundaries of the reservoir occurs. Each fracture is assumed to span the thickness of the reservoir, and the fracture network is assumed to contain no intersections formed by more than two fractures. Gravity effects are ignored, and the flow is single phase. The simulator handles wells that are horizontal (including multilaterals) or vertical and are either hydrofractured or intersected by natural fractures. All flow towards the well occurs through the fractures, except for drainage from the rock directly contacting the well bore.

Volumetric flow within the fractures and well bore is modeled as a linear (cubic law) function of the pressure difference between the recharge points and the fracture intersections. Darcy's Law is used to model the flow through the rock matrix to the recharge points in the nearby fractures. The resulting material balances at each fracture intersection and recharge point are discretized using finite difference and solved using a Newton-Raphson technique.

2. RESERVOIR FLOW SIMULATOR DEVELOPMENT

NFFLOW begins by accessing a file containing the starting and ending points of all fractures and horizontal well bores in the reservoir and determines intersection locations. For each intersection it assigns the west direction to be toward the starting point of one fracture forming the intersection and the east direction to be toward its ending point. The other fraction forming the intersection is similarly assigned south and north directions.

The resulting fracture network is represented by a collection of flow paths that intersect at points referred to as nodes. The nodes formed by the intersection of two fractures are called normal nodes, whereas nodes formed by the intersection of a well and a fracture are called well nodes. Each flow path is subdivided into segments by adjacent nodes. As each segment of the flow path drains into the next segment, it is recharged by gas from the surrounding matrix rock. Gas pressure in a segment establishes the unsteady boundary condition for modeling flow into it. Therefore, recharge of the fracture segment is determined, in part, by the pressure history in the segment.

The recharge flow is lumped to occur at the midpoint of each segment. This flow is modeled by two one-dimensional systems that represent the dynamics of flow in the matrix rock on either side of its segment. Each of these systems is assigned an effective volume based on the network geometry.

The volumetric flow rate in the fractures is modeled using the expression $Q_v = -\frac{hw^3}{12\mu}\frac{dp}{ds}$, where h is the formation thickness, w is the fracture aperture, μ is the gas

viscosity, and $\frac{dp}{ds}$ is the gas pressure gradient along the flow path. The molar gas density is given by the real gas equation of state $\rho = \frac{1}{RT}\frac{p}{Z}$, where R is the gas constant, T is the temperature, and Z is the Z-factor which is a function of p alone, since the reservoir is isothermal.

No gas accumulates at a normal node, so the material balance there is obtained by requiring that the molar inflows to that node sum to zero,

$$0 = -\left(\frac{hw^3}{12\mu}\right)_w \frac{p}{RTZ}\frac{dp}{ds}\bigg|_{P\text{-}w} + \left(\frac{hw^3}{12\mu}\right)_e \frac{p}{RTZ}\frac{dp}{ds}\bigg|_{P\text{-}e} - \left(\frac{hw^3}{12\mu}\right)_s \frac{p}{RTZ}\frac{dp}{ds}\bigg|_{P\text{-}s} + \left(\frac{hw^3}{12\mu}\right)_n \frac{p}{RTZ}\frac{dp}{ds}\bigg|_{P\text{-}n},$$

where the normal node for which a material balance is being written is labeled P and where the midpoints of the four corresponding segments that meet at node P are labeled e, w, n, and s. The nodes at the other ends of the segments are labeled E, W, N, and S respectively. The subscript, P-w, indicates the pressure gradient at node P on the w side, for instance.

By introducing the real-gas pseudopotential (potential for short),

$$\Phi = \int_0^p \frac{p'\,d'p}{\mu(p')\,Z\,(p')}, \qquad \text{(Eq. 1)}$$

and differentiating it along the flow path of each adjoining segment, the material balance at P can be written $0 = -\left(\frac{hw^3}{12}\right)_w \left(\frac{d\Phi}{ds}\right)_{P\text{-}w} + \left(\frac{hw^3}{12}\right)_e \left(\frac{d\Phi}{ds}\right)_{P\text{-}e} - \left(\frac{hw^3}{12}\right)_s \left(\frac{d\Phi}{ds}\right)_{P\text{-}s} + \left(\frac{hw^3}{12}\right)_n \left(\frac{d\Phi}{ds}\right)_{P\text{-}n}$.

Since fluid enters the flow paths only at the recharge points, the molar flow is constant between a recharge point and a node. Thus the material balance can be expressed without further approximation by $0 = -\left(\frac{hw^3}{12}\right)_w \frac{\Phi_P - \Phi_w}{.5\Delta s_w} + \left(\frac{hw^3}{12}\right)_e \frac{\Phi_e - \Phi_P}{.5\Delta s_e} - \left(\frac{hw^3}{12}\right)_s \frac{\Phi_P - \Phi_s}{.5\Delta s_s} + \left(\frac{hw^3}{12}\right)_n \frac{\Phi_n - \Phi_P}{.5\Delta s_n}$,

where $0.5\Delta s_i$ is the distance from P to the midpoint of segments i. The expression for the material balance at normal node P is more concisely written by using the fracture transmissibility $TX_i^f = \left(\frac{hw^3}{12\Delta s}\right)_i$, $i = w,e,n,s$; accordingly, the material balance at normal node P is

$$0 = 2TX_w^f(\Phi_w - \Phi_p) + 2TX_e^f(\Phi_e - \Phi_p) + 2TX_s^f(\Phi_s - \Phi_p) + 2TX_n^f(\Phi_n - \Phi_p) \quad . \qquad \text{(Eq. 2)}$$

By assumption, each segment is recharged with gas from the surrounding rock matrix, and its recharge rate depends on the pseudopotential at its respective midpoint, Φ_n, Φ_s, Φ_e, *or* Φ_w. For example consider the material balance for segment e,

$$\frac{d}{dt}\int_{V_e} \frac{1}{RT}\frac{p}{Z}\,dV = -\left(\frac{hw^3}{12\mu}\right)_e \left(\frac{1}{RT}\frac{p}{Z}\frac{\partial p}{\partial s}\right)_{e-P} + \left(\frac{hw^3}{12\mu}\right)_e \left(\frac{1}{RT}\frac{p}{Z}\frac{\partial p}{\partial s}\right)_{e-E} + \frac{Q_r^{RC}(\Phi_e)}{RT} + \frac{Q_l^{RC}(\Phi_e)}{RT},$$

where $\frac{Q_r^{RC}}{RT}$ and $\frac{Q_l^{RC}}{RT}$ are the molar recharge rates from the right and left sides of the fracture segment, respectively, as moving from start to end along the fracture. Using the pseudopotential and fracture transmissibility, the material balance for segment e becomes

$\frac{d}{dt}\int_{V_e}\frac{p}{Z}dV = 2TX_e^f(\Phi_P - \Phi_e) + 2TX_e^f(\Phi_E - \Phi_e) + Q_r^{RC} + Q_l^{RC}$. Approximate the integral by $V_e\left(\frac{p}{Z}\right)_e$, and approximate the time derivative by a backward difference to obtain

$$\frac{V_e}{\Delta t_{n+1}}\left[\left(\frac{p}{Z}\right)_e^{n+1} - \left(\frac{p}{Z}\right)_e^{n}\right] = 2TX_e^f\left(\Phi_P^{n+1} + \Phi_E^{n+1} - 2\Phi_e^{n+1}\right) + Q_r^{RC}\left(\Phi_e^{n+1}\right) + Q_l^{RC}\left(\Phi_e^{n+1}\right) \quad , \qquad \text{(Eq. 3)}$$

where Δt_{n+1} is the time interval between t_n and t_{n+1}.

The material balance at the well nodes is similar to the balance at a normal node except that the pressure (hence potential) is uniform for all nodes and recharge points that are a part of the well. For a pressure controlled well, the pressure is specified by the user and the total inflow to the well represents the production rate for the well. In the case of a rate controlled well, the total inflow to the well is required to sum to a user specified value (boundary condition) and the well potential is an unknown to be solved for. The well material balance is

$$\frac{d}{dt}\int_{V_{WB}}\frac{p}{RT\,Z}dV + \rho_{sc}\,Q_{Vsc} = \sum_{k'}\left(\frac{Q_r^{rc}}{RT} + \frac{Q_l^{rc}}{RT}\right)_{k'} + \sum_{j'}\left[\left(\frac{hw^3}{12}\right)_l\left(\frac{P}{Z\mu}\frac{dP}{ds}\right)_{j'-l} - \left(\frac{hw^3}{12}\right)_r\left(\frac{P}{Z\mu}\frac{dP}{ds}\right)_{j'-r}\right],$$

where k' is summed over the well segments, j' is summed over the intersecting fractures, and the indices r an l indicate properties associated with the fracture segments intersecting the horizontal well from the right and left, respectively. The integral represents the rate of gas accumulation in the horizontal well, ρ_{sc} is the molar density at standard conditions, and Q_{Vsc} is the volumetric flow rate measured at standard conditions. As with normal nodes, the well bore material balance can be written in terms of the pseudopotential and the fracture transmissibility. Then, by approximating the integral and backward differencing in the same manner as for the normal nodes, the well bore material balance becomes

$$0 = \frac{-V_{WB}}{\Delta t_{n+1}}\left[\left(\frac{p}{Z}\right)_{WB}^{(n+1)} - \left(\frac{p}{Z}\right)_{WB}^{n}\right] - Q_{WB} + \sum_{k'}\left(Q_r^{RC} + Q_l^{RC}\right)_{k'} + 2\sum_{j'}\left[TX_r^f\left(\Phi_r - \Phi_{WB}\right) + TX_l^f\left(\Phi_l - \Phi_{WB}\right)\right]_{j'},$$

(Eq. 4)

where Φ_{WB} is the well bore potential, Φ_r and Φ_l are the potentials at the recharge points of the right and left segments of the intersecting fractures, respectively, V_{WB} is the volume of the horizontal well bore, and Q_{WB} is the molar flow of gas, $\frac{p_{sc}TQ_{Vsc}}{T_{sc}}$.

The rock matrix is partitioned into blocks by the fractures. Each block is further divvied into fractions, one for each bounding fracture segment. The fraction of a block that feeds its adjacent fracture segment is roughly proportional to the length of that fracture segment and is characterized only by its effective volume. No gas flows between effective volumes. Once the effective volume of the rock matrix recharging a fracture segment is established, the flow path of the gas through the matrix is treated as one-dimensional flow.

The continuity equation for flow in porous media is $0 = A_c\frac{\partial}{\partial t}(\phi\rho) + \frac{\partial}{\partial x}\left(A_c\,\rho\bar{u}\right)$, where A_c is the cross-sectional area of the effective volume, φ is the porosity of the matrix rock, and $\bar{u}$ is the superficial or darcy velocity. Using the equation of state for ρ, Darcy's Law for $\bar{u}$, the

pseudopotential definition, and the fact that RT is constant gives $0 = A_c \frac{\partial}{\partial t}\left(\phi \frac{p}{Z}\right) - \frac{\partial}{\partial x}\left(A_c\, k_m \frac{\partial \Phi}{\partial x}\right)$, where k_m is the matrix permeability.

Each effective volume is discretized into n_b cells, each centered at x_m with length Δx_m where m=1,...n_b. The boundaries of cell m are at $x_{m-1/2}$ and $x_{m+1/2}$. The size of n_b is larger for wider effective volumes, so that all Δx_1's are about the same value. The continuity equation is integrated over each cell in each block with respect to x from $x_{m-1/2}$ to $x_{m+1/2}$, yielding for cell m $0 = \frac{d}{dt}\int_{m-1/2}^{m+1/2} A_c \phi\left(\frac{p}{Z}\right) dx - \left(A_c\, k_m \frac{\partial \Phi}{\partial x}\right)_{x_{m+1/2}} + \left(A_c\, k_m \frac{\partial \Phi}{\partial x}\right)_{x_{m-1/2}}$. The integral is approximated by $V_m\left(\frac{p}{Z}\right)_m$ where V_m is the pore volume of cell m, and the flow terms are approximated by $\pm 2\left(k_m A_c\right)_{m\pm 1/2} \frac{\Phi_{m\pm 1} - \Phi_i}{\Delta x_m + \Delta x_{m\pm 1}}$, where the plus sign holds at $x_{m+1/2}$ and the minus sign at $x_{m-1/2}$. These expressions for the flow terms hold at all cell boundaries except $x_{1/2}$ and $x_{n_b+1/2}$. The flow at $x_{1/2}$, the recharge flow Q^{RC}, is given by $2\left(k_m\ A_c\right)_{1/2} \frac{\Phi_1 - \Phi_0}{\Delta x_1}$, where Φ_0 is the potential at the recharge point in the adjacent fracture segment, (i.e. Φ_n, Φ_s, Φ_e, *or* Φ_w). The flow at $x_{n_b+1/2}$ is zero by the assumption that no flow among effective volumes occurs. Finally, by defining $TX_{n_b+1/2} = 0$, $TX_{1/2} = 2\left(k_m A_c\right)_{1/2} / \Delta x_1$, and $TX_{m+1/2} = 2\left(k_m A_c\right)_{m+1/2} / \left(\Delta x_m + \Delta x_{mi+1}\right)$ $m = 1..., n_b$, the continuity equation for flow through any cell m becomes $0 = \frac{d}{dt}\left[V_m\left(\frac{p}{Z}\right)_m\right] - TX_{m+1/2}\left(\Phi_{m+1} - \Phi_m\right) + TX_{m-1/2}\left(\Phi_m - \Phi_{m-1}\right)$ $m = 1,..., n_b$. The finite difference equations for the rock matrix are completed by using backward differencing

$$0 = \frac{1}{\Delta t_{n+1}}\left[V_m^{n+1}\left(\frac{p}{Z}\right)_m^{n+1} - V_i^n\left(\frac{p}{Z}\right)_m^n\right] - TX_{m+1/2}\left(\Phi_{m+1}^{n+1} - \Phi_m^{n+1}\right) + TX_{m-1/2}\left(\Phi_m^{n+1} - \Phi_{m-1}^{n+1}\right),\ m = 1,..., n_b. \quad \text{(Eq. 5)}$$

Unless the gas pressure is extremely high the change in pore volume with pressure is small compared to the gas compressibility; therefore, the V_m are treated as constants. The independent variables in equations 2 through 5 are the pseudopotentials. Each $\frac{P}{Z}$ is an implicit function of the pseudopotential through equation 1.

Equations 2 through 5 are solved using the Newton-Raphson method. The residual for the material balance at a normal node P is $R_P^{(k)} = 2TX_w^f\left(\Phi_w^{(k)} - \Phi_P^{(k)}\right) + 2TX_e^f\left(\Phi_e^{(k)} - \Phi_P^{(k)}\right) + 2TX_s^f\left(\Phi_s^{(k)} - \Phi_P^{(k)}\right) + 2TX_n^f\left(\Phi_n^{(k)} - \Phi_P^{(k)}\right)$, where (k) indexes the iteration and P references all normal nodes. The residual of the material balance along a fracture segment i is $R_i^{(k)} = 2TX_i^f\left(\Phi_P^{(k)} + \Phi_j^{(k)} - 2\Phi_i^{(k)}\right) + Q_r^{RC(k)} + Q_l^{RC(k)} - \frac{V_{fi}}{\Delta t_{n+1}}\left[\left(\frac{p}{Z}\right)_i^{(k)} - \left(\frac{p}{Z}\right)_i^n\right]$, where i=n,s,e,w and j=N,S,E,W. The residual for the well bore material balance is

$R_{WB}^{(k)} = 2\sum_{j'}\left[TX_r^f\left(\Phi_r^{(k)} - \Phi_{WB}^{(k)}\right) + TX_l^f\left(\Phi_l^{(k)} - \Phi_{WB}^{(k)}\right)\right]_{j'} + \sum_{k'}\left(Q_r^{RC\,(k)} + Q_l^{RC\,(k)}\right)_{k'} - \frac{V_{WB}}{\Delta t_{n+1}}\left[\left(\frac{p}{Z}\right)_{WB}^{(k)} - \left(\frac{p}{Z}\right)_{WB}^{n}\right] - Q_{WB}$. The residual for the material balance in cell m of an effective volume in the rock matrix is

$R_m^{(k)} = \frac{V_m}{\Delta t_{n+1}}\left[\left(\frac{p}{Z}\right)_m^{(k)} - \left(\frac{p}{Z}\right)_m^{n}\right] - TX_{m+1/2}\left(\Phi_{m+1}^{(k)} - \Phi_m^{(k)}\right) + TX_{m-1/2}\left(\Phi_m^{(k)} - \Phi_{m-1}^{(k)}\right)$, where m references all cells in all effective volumes. Define the update increment $\delta\Phi_l^{(k+1)} = \Phi_l^{(k+1)} - \Phi_l^{(k)}$, and form the Newton-Raphson update expression from each residual:

$$-R_P^{(k)} = 2TX_w^f\left(\delta\Phi_w^{(k+1)} - \delta\Phi_P^{(k+1)}\right) + 2TX_e^f\left(\delta\Phi_e^{(k+1)} - \delta\Phi_P^{(k+1)}\right) + 2TX_s^f\left(\delta\Phi_s^{(k+1)} - \delta\Phi_P^{(k+1)}\right) + 2TX_n^f\left(\delta\Phi_n^{(k+1)} - \delta\Phi_P^{(k+1)}\right), \quad \text{(Eq. 6)}$$

$$-R_i^{(k)} = 2TX_i^f\left(\delta\Phi_P^{(k+1)} + \delta\Phi_j^{(k+1)} - 2\delta\Phi_i^{(k+1)}\right) + \left(\frac{\partial Q_r^{RC}}{\partial\Phi}\right)_i^{(k)}\delta\Phi_i^{(k+1)} + \left(\frac{\partial Q_l^{RC}}{\partial\Phi}\right)_i^{(k)}\delta\Phi_i^{(k+1)} - \frac{V_{fi}}{\Delta t_{n+1}}\frac{\partial}{\partial\Phi_i}\left(\frac{P}{Z}\right)^{(k)}\delta\Phi_i^{(k+1)}, \quad \text{(Eq. 7)}$$

$$-R_{WB}^{(k)} = 2\sum_{j'}\left[TX_r^f\left(\delta\Phi_r^{(k+1)} - \delta\Phi_{WB}^{(k+1)}\right) + TX_l^f\left(\delta\Phi_l^{(k+1)} - \delta\Phi_{WB}^{(k+1)}\right)\right]_{j'} + \sum_{k'}\left[\left(\left(\frac{\partial Q_r^{RC}}{\partial\Phi}\right)_{WB}^{(k)} + \left(\frac{\partial Q_l^{RC}}{\partial\Phi}\right)_{WB}^{(k)}\right)\delta\Phi_{WB}^{(k+1)}\right]_{k'} - \frac{V_H}{\Delta t_{n+1}}\frac{\partial}{\partial\Phi_{WB}}\left(\frac{p}{Z}\right)^{(k)}\delta\Phi_{WB}^{(k+1)}, \quad \text{(Eq. 8)}$$

and

$$-R_m^{(k)} = \left(\frac{V_m}{\Delta t_{n+1}}\right)\left[\frac{\partial}{\partial\Phi_m}\left(\frac{p}{Z}\right)\right]^{(k)}\delta\Phi_m^{(k+1)} - TX_{m+1/2}\left(\delta\Phi_{m+1}^{(k+1)} - \delta\Phi_m^{(k+1)}\right) + TX_{m-1/2}\left(\delta\Phi_m^{(k+1)} - \delta\Phi_{m-1}^{(k+1)}\right). \quad \text{(Eq. 9)}$$

If node P is either the first or last intersection of a fracture, then equation 7 is modified to reflect that no node j exists. The update increment is zero, $\delta\Phi_l^{(k+1)} = 0$, if it refers to a potential along a well bore and if that well is pressure controlled. The compressibility of the fluid, c_g, is used to evaluate the derivative, $\frac{\partial}{\partial\Phi}\left(\frac{P}{Z}\right) = \frac{\partial}{\partial P}\left(\frac{P}{Z}\right)\left(\frac{\partial\Phi}{\partial P}\right)^{-1} = \mu c_g$. The derivative, $\frac{\partial Q^{RC}}{\partial\Phi} = TX_{1/2}\left(\frac{\partial\Phi_1}{\partial\Phi_0} - 1\right)$, is found by solving the set of equations representing the converged residual expression for flow through the rock matrix, $0 = \frac{\left(V\mu c_g\right)_i}{\Delta t_{n+1}}\frac{\partial\Phi_i}{\partial\Phi_0}\Big|^{n+1} - TX_{i+1/2}\left[\frac{\partial\Phi_{i+1}}{\partial\Phi_0}\Big|^{n+1} - \frac{\partial\Phi_i}{\partial\Phi_0}\Big|^{n+1}\right] + TX_{i-1/2}\left[\frac{\partial\Phi_i}{\partial\Phi_0}\Big|^{n+1} - \frac{\partial\Phi_{i-1}}{\partial\Phi_0}\Big|^{n+1}\right], i = 1\ldots n_b$.

The solution procedure first calculates the residuals, and if they are not sufficiently close to zero, it uses equation 9 to solve for the pseudopotentials throughout the rock matrix and allow the determination of every recharge flow, Q^{RC}. Then, equations 6, 7, and 8 are solved to determine the pseudopotential update increments and pseudopotentials in the fractures and well

bore(s). The residuals are computed, and the algorithm cycles again until convergence is achieved.

3. RESULTS

A 24 hour well test analysis of a gas field in Oriskany Sandstone was simulated by NFFLOW. The reservoir contains a core-measured matrix permeability of 0.01 md and a core measured matrix porosity of 0.3%. The fracture aperture is assumed to be a universal 0.016 cm. The reservoir pressure was initially 1682 psi (11600 kPa) and finally 1670 psi (11510 kPa). As indicated by the dark line, the well has about 1000 ft (305 m) of lateral penetration, and the wellhead is indicated by the square at one end of the lateral. As detected with a CBIL log, 205 fractures intersect the lateral. Assuming vertical homogeneity in the reservoir, the fracture pattern used by NFFLOW is shown in Figure 1.

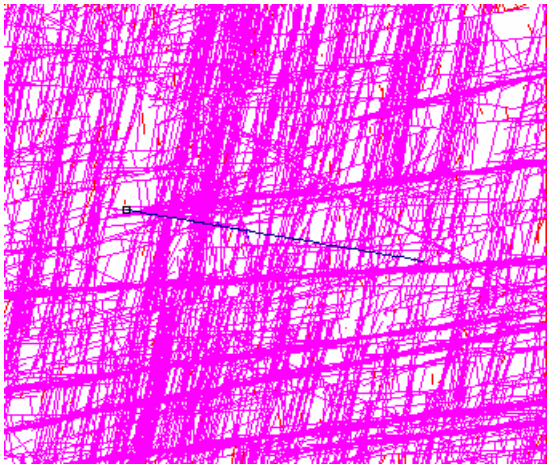

FIGURE 1. Well and Fracture Pattern

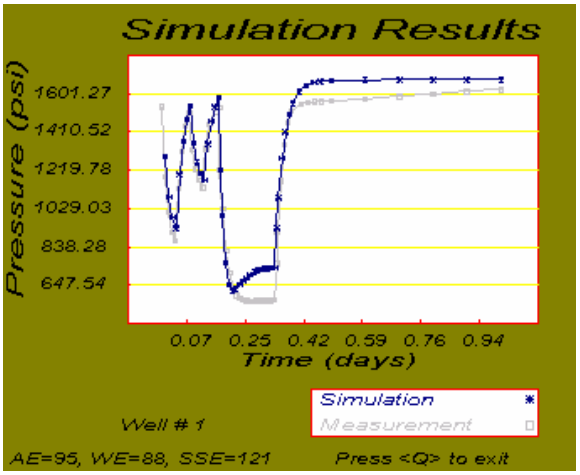

FIGURE 2. Wellhead Pressure

The gray line in Figure 2 indicates the measured wellhead pressure as the flow was controlled over one day. The NFFLOW pressure prediction, as indicated by the darker line, deviates from the measured only during the fastest drawdown and subsequent recovery. The deviation during drawdown can be explained by not accounting sufficiently for the fracture aperture occlusion caused by well damage, or by incorrect rock porosity or permeability. The deviation during recovery could be caused by the simulated fracture network being better connected to the well than the actual fracture network. AE, WE, and SSE refer respectively to average absolute error, pressure weighted average absolute error, and standard deviation of the error over the duration of the test.

The simulation required 15 minutes on a standard desktop PC. Although not done in this case, NFFLOW could have been rerun after invoking an ancillary program to account for well damage, or it could have been rerun after changing the rock characteristics. Also, NFFLOW could have been rerun after another associated program called FRACGEN had been used to generate a second representation of the fracture network, or a third, or a fourth. Presumably, a near perfect match with historic data could have been achieved with enough trial and error.

However, no matter the fracture network, or aperture distribution, or rock porosity or permeability, none of the trials would have affected NFFLOW or changed its assumptions and approach. Fractures are accessed by their starting and ending points. Intersections are found and indexed. The pseudopotential is used, so compressible fluids, either gas or liquid, are handled. Using Newton-Raphson it solves the material balance along the fractures and well bore and couples them to the flow in the surrounding rock matrix through the potential at the recharge point.

4. ACKNOWLEDGEMENT

The authors wish to thank Mark L. McKoy for generating the fracture network and for his help in preparing the article, and Edward J. Boyle for his help in preparing the article.

REFERENCES

Al-Hussainy, R., H.J. Ramey, Jr., and P.B. Crawford (1966a), The flow of real gases through porous media, *J.Pet.Tech Trans. AIME., May*, 624-636.

Al-Hussainy, R. and H.J. Ramey, Jr. (1966b), Application of real gas flow theory to well testing and deliverability forecasting, *J.Pet.Tech Trans. AIME., May*, 637-642.

Baecher, G.B., N.A. Lanney, and H.H. Einstein (1977), Statistical descriptions of rock properties and sampling, *Proceedings of the 18th U.S. Symposium on Rock Mechanics, AIME*, p.5C1, 1-8.

Gervais, F., J.P. Chiles, and S. Gentier (1995), Geostatistical analysis and hierarchial modeling of a fracture network in a stratified rock mass, in *Fractured and Jointed Rock Masses* , edited by Myer et al., A.A. Balkema, Rotterdam, pp 153-159.

Long, J.C.S., J.S. Remer, C.R. Wilson, and P.A. Witherspoon (1982), Porous media equivalents for networks of discontinuous fractures, *Water Resources Research*, *18, no. 3*, 645-658.

McKoy, M. L. and W. N. Sams (1997), Tight gas reservoir simulation: modeling discrete irregular strata-bound fracture networks and network flow, including dynamic recharge from the matrix, paper presented at Natural Gas Conference, US DOE, Houston TX, March 24-27.

Park, Y.C., W. M. Sung, and S.J. Kim (2002), Development of a FEM reservoir model equipped with an effective permeability tensor and its application to naturally fractured reservoirs, *Energy Sources, 24 (6)*, 531-542.